THE CONCRETE NZ CONFERENCE 2018
PROGRESS THROUGH COLLABORATION
Claudelands, Hamilton | 11 – 13 October 2018

DEFORMATION CAPACITY OF CONCRETE WALLS: RESEARCH FINDINGS FOR BOTH OLD AND NEW DESIGN PRACTICE

ALEX SHEGAY, TONGYUE ZHANG, SIGNY CROWE, KEN ELWOOD, RICK HENRY

Department of Civil & Environmental Engineering, University of Auckland

SUMMARY

Recent research results are presented that investigate the seismic performance of both singly reinforced concrete walls in existing buildings and modern ductile RC walls subjected to high axial loads. Current assessment and design provisions do not adequately address these wall types and new models are presented to estimate failure mode and deformation capacity. The criteria to estimate walls vulnerable to axial failure could be implemented into seismic assessment guidelines to define those with a severe structural weakness. In addition, the refined model to estimate deformation capacity for ductile walls should be used in both new design and seismic assessment.

INTRODUCTION

Damage to concrete walls during the Canterbury earthquakes led to significant research related to the seismic assessment and design of RC walls (CERC 2012, Sritharan et al. 2014). Recent research at the University of Auckland has addressed the lack of experimental data of two common typologies of walls:

- Singly reinforced walls with non-ductile detailing representative of 1950-1970s era.
- Modern ductile RC walls subjected to high axial loads.

Tests of existing singly reinforced wall detailing showed that sudden axial failure may occur with only modest axial loads and tests of ductile wall detailing showed that deformation capacity significantly reduced as the axial load increased. The failure mode and deformation capacity of these walls was not well represented by current seismic assessment and design provisions that were developed and verified against experimental data of walls with relatively low axial loads. Improved models were developed that are suitable for implementation in future revisions to seismic assessment guideline and concrete design standards.

EXISTING WALLS

Typical detailing of concrete walls in pre-1970s multi-storey buildings were analysed with most exhibiting non-ductile detailing, i.e. thin cross-section, single layer of reinforcement, light reinforcement content, and absence of confinement reinforcement (Zhang et al. 2018a). An experimental study was conducted to assess the seismic performance these types of walls and led to assessment of unconfined walls vulnerable to axial failure (through the thickness failure).

Experimental Tests

The experimental program consisted of four full-scale concrete walls designed in accordance with old construction practice (Zhang et al. 2018b). The test walls had a length of 1920 mm, height of 3840 mm, and a thickness of either 150 mm or 200 mm, as shown in Figure 1. The test walls had a single layer of distributed reinforcement in both horizontal and vertical directions, which corresponded to a reinforcement ratio of around 0.25%. The test walls were subjected to a combination of constant axial load and cyclic lateral load. In addition to variations in thickness the axial load ratio applied to the test walls was varied from 3.5% to 10%, which falls into the common range of axial loads carried by walls in real buildings.

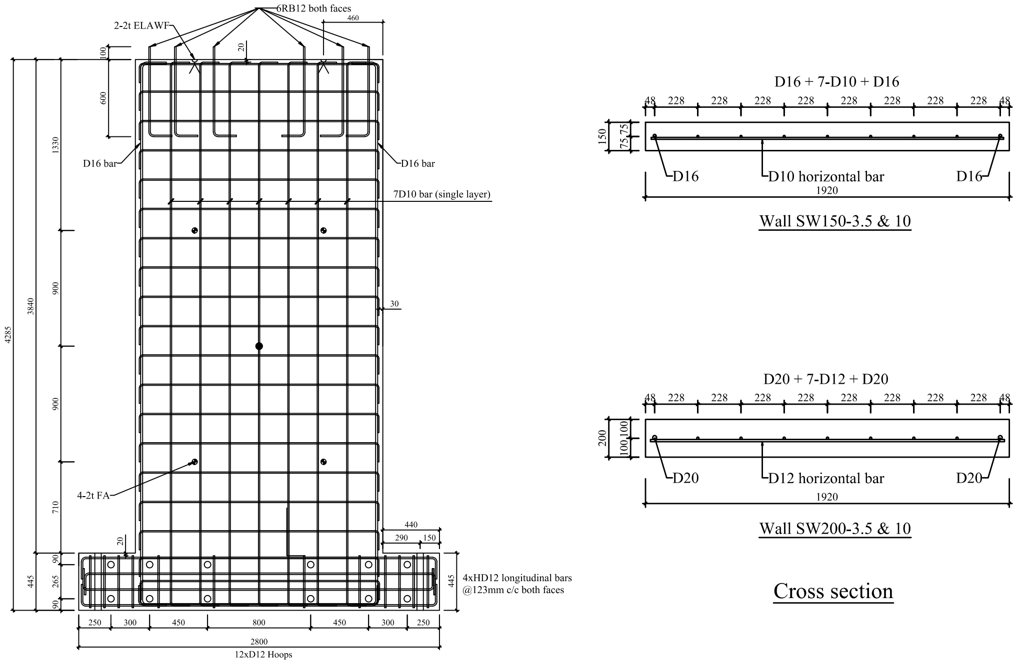

Figure 1 Details of singly reinforced test walls.

The test walls exhibited limited deformation capacity along with the development of only two or three dominant flexural cracks. Due to the lack of confinement reinforcement, concrete crushed soon after the wall reached the peak lateral strength. The axial load magnitude was critical to the failure mode and performance of the test walls. With the increase in applied axial load ratio from 3.5% to 10%, wall failure transformed from longitudinal reinforcement fracture to sudden axial compression failure, as shown in Figure 2. The axial compression failure was triggered by crushing and shifting in the out-of-plane direction across the entire wall length, resulting in a total loss of axial load carrying capacity.

West East

(a) Bar fracture of SW150-3.5 (b) Axial failure of wall SW200-10

Figure 2 Failure of singly reinfroced test walls.

Identifying Axial Failure

The axial failure of test walls subjected to 10% axial load highlighted the vulnerability of non-ductile walls in existing buildings. The lack of transverse reinforcement to provide confinement to the concrete, led to sudden failure due to loss of axial load carrying capacity when initial crushing occurred. The sudden axial failure is likely to occur at small lateral drifts and is therefore significant to the assessed seismic capacity of existing buildings. The axial failure of non-ductile walls is characterised by the development of a diagonal failure plane through the wall thickness and sudden crushing across the entire length of the wall (referred to as through-the-thickness or TTT failure) and therefore fits the criteria of a severe structural weakness (SSW).

The test results in addition to a database of other relevant past wall tests was used to identify criteria that determined when through-the-thickness axial failure was likely to occur. Previous experimental research stressed the influence of axial load and confinement reinforcement on the transition of failure modes in concrete walls (Alarcon et al. 2014, Hube et al. 2014, Su and Wong 2007). The results of test walls exhibiting different failure modes are plotted in Figure 3. Both singly and doubly reinforced walls with no confinement reinforcement (s/t = ∞) were observed to be prone to axial failure when axial load ratios exceeded 8%. For walls with confinement reinforcement, there was an increase in the axial loads that could be sustained without axial failure when the spacing of the transverse reinforcement to wall thickness (s/t) was less than 1. Walls with large axial load ratios (greater than 30%) have not been extensively tested, but appear to be prone to axial failure regardless of detailing.

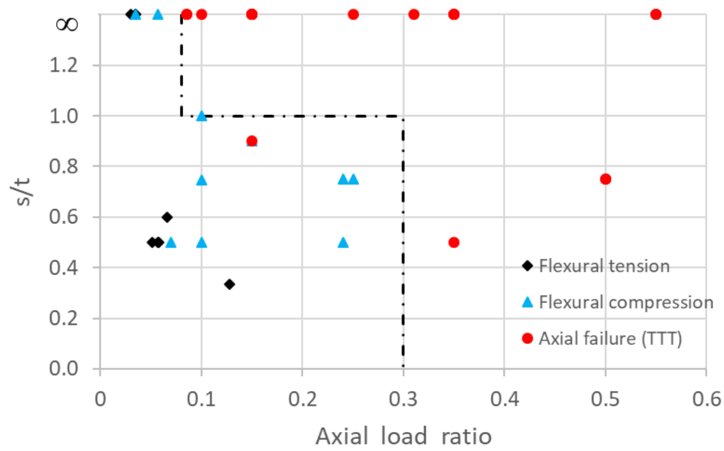

Figure 3 Proposed axial failure model for capacity assessment.

Based on the analysis to the test wall data, the following criteria was defined to identify walls where the behaviour was controlled by axial failure and SSW criteria should apply (also plotted as dot-dash line in Figure 3):

$$\frac{(A_s - A_s')f_y + N^*}{t_w l_w f_c'} > 0.3 \qquad \text{Eq. 1}$$

$$s/t_w > 1 \quad \text{and} \quad \frac{(A_s - A_s')f_y + N^*}{t_w l_w f_c'} > 0.08 \qquad \text{Eq. 2}$$

Where A_s and A'_s are area of non-prestressed tension and compression reinforcement, respectively, N^* is the axial load, f_y is the probable yield strength of longitudinal reinforcement,

f_c' is the probable concrete compression strength, t_w is the wall thickness, l_w is the wall length, and s is the vertical spacing of closed hoops or cross-ties in the boundary area.

MODERN DUCTILE WALLS

Several RC walls designed to modern standards (post 1970s construction) sustained unexpected levels damage in the 2010/2011 Canterbury earthquakes. Recommendations for the design of RC walls were proposed in the SESOC Interim Design Guidelines (SESOC 2013) and the Canterbury Earthquake Royal Commission reports (CERC 2012). A number of recommendations have been adopted in the third amendment of the New Zealand Concrete Structures Standard (NZS 3101:2006-A3), published in 2017. Of particular interest was the introduction of a wall axial load limit of 30% of the total wall compression capacity. It was of interest to investigate the performance of walls as the imposed axial load approached the new design limit, specifically the effects on wall deformation capacity.

Experimental Tests

Three half-scale reinforced concrete walls were designed and tested at the University of Auckland with the primary objective of investigating the compatibility of wall performance over a range of axial load demands with the existing NZS 3101:2006-A3 curvature ductility (K_d) demand limits in §2.6.1.3.4. Cross sections for the test walls are shown in Figure 4. The walls were subjected to axial loads of 10% (Wall A10), 14% (Wall A14) and 20% (Wall A20) of the total wall axial compression capacity. The plastic hinges of the walls were detailed according to the 'Ductile' plastic hinge region provisions of NZS 3101:2006-A3. The detailing included a fully confined compression zone and cross-ties on all web longitudinal reinforcement. Further detail of the experiment program are published in Shegay et al. (2018).

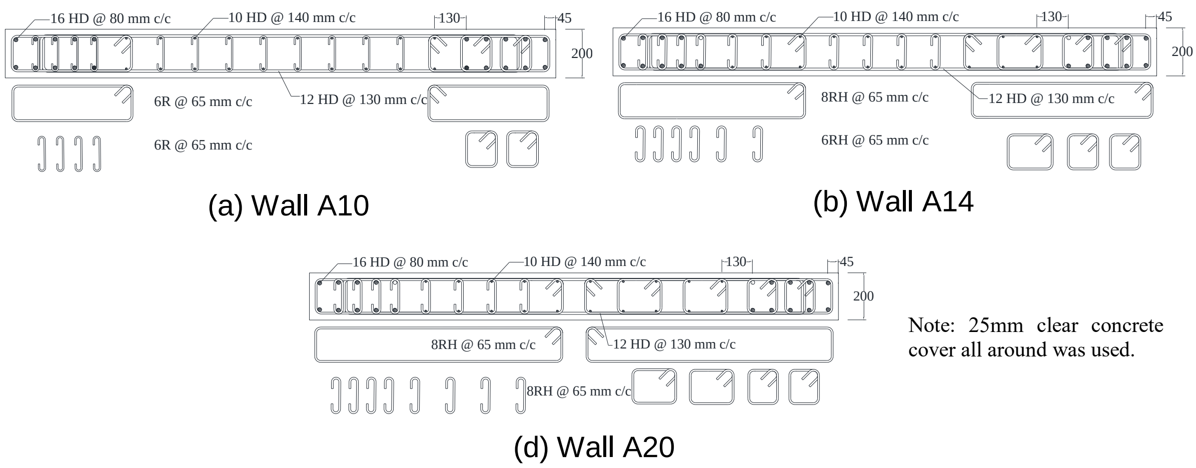

Figure 4: Cross-sections and reinforcement detailing of the test walls.

The damage states of the wall end regions following loss of lateral and axial load carrying capacity is show in Figure 5. All three specimens exhibited a similar sequence of damage characterized by well distributed cracking followed by spalling of cover concrete at the wall end regions, reinforcement buckling and crushing of the confined core. Similarly to singly reinforced walls, the ductile walls moved out-of-plane when axial load carrying capacity was lost. It was observed that with higher axial load, the amount and the extent of spalling (along the length and up the height of the wall) increased, while the width of flexural cracks and the severity of reinforcement buckling decreased. Fracture of longitudinal reinforcement was only observed in Wall A10.

A10 A14 A20

Figure 5: Damage state following loss of lateral and axial load carrying capacity.

<u>Deformation capacity</u>

The three tests demonstrated that increasing axial load correlated to a reduction of deformation capacity of the wall plastic hinge region, with Wall A10, A14 and A20 achieving plastic rotation capacities of 0.032, 0.027 and 0.021 rad, respectively. This reduction is not currently reflected in the deformation limits in NZS 3101:2006-A3. Though previous models have been proposed to relate deformation capacity directly to the level of axial load demand, it is understood that the wall deformation capacity is fundamentally governed by strain capacities in the concrete and reinforcement. It follows then that axial load is only one of several parameters (including material properties, longitudinal reinforcement ratio, cross-section geometry) that can affect the compression strain demand in the end region. Therefore, a new deformation capacity model was proposed that is a function of the more comprehensive c/L_w parameter (ratio of neutral axis length to wall length), that appropriately considers the compressive demand in the end region.

To develop this model, the results from the above experimental program were combined with a more comprehensive dataset of previously tested walls with similar characteristics that complied with NZS 3101:2006-A3 'Ductile' detailing provisions. The experimental curvature ductility capacity for each of the walls is plotted against their respective c/L_w ratios in Figure 6a and Figure 6b, corresponding to plastic hinge length definitions of NZS 3101:2006-A3 and the New Zealand Assessment Guidelines (MBIE 2017), respectively. The existing K_d limit in NZS 3101:2006-A3 for 'Ductile walls with confined boundary elements' is also shown. Two trends in the data are observed: (i) the curvature ductility capacity reduces with increasing c/L_w ratio and (ii) the curvature ductility capacity reduces with increasing transverse reinforcement spacing to longitudinal bar diameter ratio (s/d_b). The invariable nature of the existing NZS 3101:2006 K_d limits means that these trends are not properly accounted for. As a result, a number of walls with a $c/L_w \geq 0.25$ (i.e., high compression demand) or $s/d_b > 5$ fall below the plotted NZS 3101:2006-A3 limit. This observation suggests that walls designed close to the existing NZS 3101:2006 K_d limits may in actuality not possess the deformation capacity required to meet the design deformation demand.

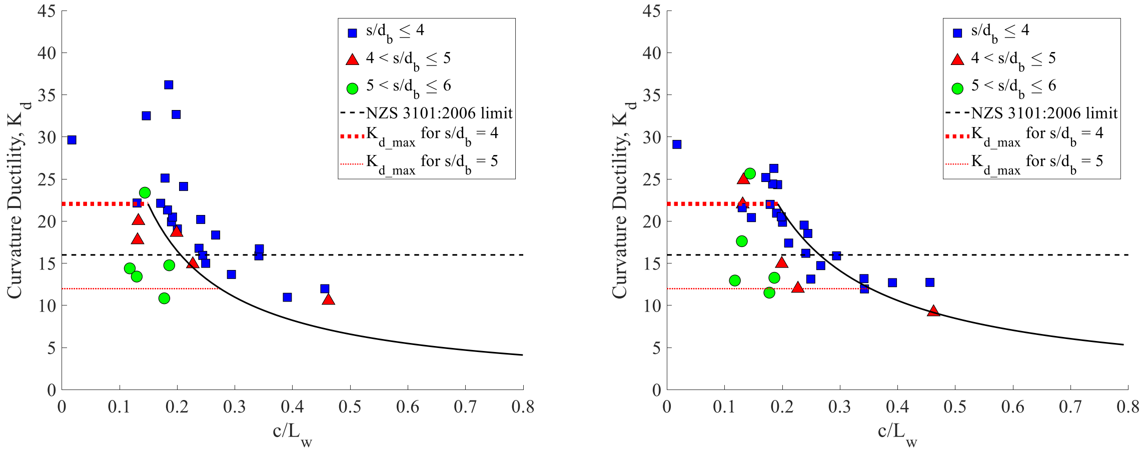

(a) (b)

Figure 6: Proposed deformation capacity models for (a) design demand limits in NZS 3101:2006-A2 and (b) capacity assessment limits in NZ Assessment Guideline.

To address this shortcoming a mechanics based model was developed that accounts for both of the K_d trends described above. Curvature ductility is defined as the maximum curvature normalized by the yield curvature. By substituting the NZS 3101:2006-A3 definition of wall yield curvature ($\phi_y = \frac{2\varepsilon_y}{L_w}$, where ε_y is the longitudinal reinforcement yield strain and L_w is the length of the wall, §2.6.1.3.4) and assuming maximum curvature, ϕ_{max}, is governed by compression failure (i.e., $\phi_{max} = \frac{\varepsilon_{cm}}{c}$, where ε_{cm} is a limiting compression strain), an expression for curvature ductility can be derived as a function of c/L_w:

$$K_d = \frac{\varepsilon_{cm}}{2\varepsilon_y\left(\frac{c}{L_w}\right)} \leq K_{d\_max} \qquad \text{Eq. 3}$$

K_{d_max} in the above equation provides an upper bound the K_d limit by acknowledging that at low c/L_w ratios the section deformation capacity will transition from being governed by the crushing of concrete to being governed by buckling or fracture of the longitudinal reinforcement. The proposed K_{d_max} values are summarised in Table 1 and were derived based on Euler buckling mechanics as extended by Rodriguez et al. (1999) and Moyer and Kowalsky (2003). The ε_{cm} limits were selected to provide the most suitable lower bound and probable estimate of curvature ductility, corresponding to the proposed design demand and assessment capacity limits, respectively. The resulting limit models are computed using Eq 3 and are plotted on Figure 6a and 6b. It is clear from these figures that the proposed limits do a better job at accounting for the variation in deformation capacity over the range of c/L_w and s/d_b ratios, than the existing NZS 3101:2006 limits.

Table 1: Concrete compressive strain limits and K_{d_max} limits for the proposed model in Eq 3

Concrete strain limit for assessment (probable)	$\varepsilon_{cm} = 0.018$
Concrete strain limit for design (lower bound)	$\varepsilon_{cm} = 0.014$
K_{d_max}	12 for $s/d_b \geq 5$ 22 for $s/d_b \leq 4$ Linear interpolation for $4 \leq s/d_b \leq 5$

CONCLUSIONS

New models were presented to estimate failure mode and deformation capacity of walls in both existing and new buildings. The criteria to estimate walls vulnerable to axial failure could be implemented into seismic assessment guidelines to define those with a severe structural weakness. In addition, the refined model to estimate deformation capacity for ductile walls should be used in both new design and seismic assessment, especially for walls where large axial loads are applied and current provisions are unconservative.

REFERENCES

Alarcon, C., Hube, M. A., & de la Llera, J. C. (2014). Effect of axial loads in the seismic behavior of reinforced concrete walls with unconfined wall boundaries. *Engineering Structures*, 73, 13-23.

CERC, (2012): Volume 2: The Performance of Christchurch CBD Buildings. Canterbury Earthquakes Royal Commission. Christchurch, Auckland.

Hube, M. A., Marihuén, A., de la Llera, J. C., & Stojadinovic, B. (2014). Seismic behavior of slender reinforced concrete walls. *Engineering Structures*, 80, 377-388.

MBIE, (2017): The seismic assessment of existing buildings: technical guidelines for engineering assessment. Part C5 – Concrete Buildings. Joint publication of NZSEE, SESOC, NZGS, MBIE, and EQC, Wellington, New Zealand.

Moyer MJ and Kowalsky MJ, (2003): Influence of tension strain on buckling of reinforcement in concrete columns. *ACI Structural Journal*, **100**(1), 75–85.

NZS 3101:2006, (2017): *Concrete Structures Standard Part 1- The Design of Concrete Structures (Amendment No. 3)*. Standards New Zealand, Wellington, New Zealand.

Rodriguez EM, Botero JC, and Villa J, (1999): Cyclic stress-strain behavior of reinforcing steel including effect of buckling. *Journal of Structural Engineering*, **125**(6), 605–612.

SESOC (Structural Engineering Society New Zealand Inc.), (2013): Interim Design Guidance: Design of Conventional Structural Systems Following the Canterbury Earthquakes.

Shegay A V., Motter CJ, Elwood KJ, Henry RS, Lehman DE, and Lowes LN, (2018): Impact of axial load on the seismic response of rectangular walls. *Journal of Structural Engineering*, **144**(8), 1–32.

Sritharan, S., Beyer, K., Henry, R. S., Chai, Y. H., Kowalsky, M., & Bull, D. (2014). Understanding poor seismic performance of concrete walls and design implications. *Earthquake Spectra*, 30(1), 307-334.

Su, R. K. L., & Wong, S. M. (2007). Seismic behaviour of slender reinforced concrete shear walls under high axial load ratio. *Engineering Structures*, 29(8), 1957-1965.

Zhang, T., Elwood, K. J., & Henry, R. S. (2018a). Testing of reinforced concrete walls in pre-1970s multi-storey buildings. Proceedings of the 11th U.S. National Conference on Earthquake Engineering, Los Angeles, California, June 25-29.

Zhang, T., Elwood, K. J., & Henry, R. S. (2018b). Testing of singly reinforced concrete walls used in existing buildings. Proceedings of 2018 NZSEE conference, Auckland, April 13-15.